Source Characteristics of Mining-Induced Seismicity from Moment-Tensor Analysis and Spatio-Temporal Relationships

E. Richardson, A.A. Nyblade Department of Geosciences, Pennsylvania State University, USA
W.R. Walter, A.J. Rodgers Lawrence Livermore National Laboratory, USA

Mining-induced seismicity particularly interests seismologists who study earthquake physics because hard rock underground mines represent the best environment for studying small events (moment magnitude -2 ≤ M ≤ 3.5) whose dimensions are near to or below the detection threshold of most surface-based seismic arrays. We have inverted for the moment tensors of 17 events of 1.0 ≤ M ≤ 3.2 from the Far West Rand gold-mining region of South Africa. These events occurred at 1-4 km depth and were recorded locally by four networks of 102 three-component geophones installed at depth throughout the mines, as well as regionally by a surface deployment of 80 broadband seismometers. The moment tensors of these events are consistent with purely double-couple solutions. We assert that these events are proxies for natural tectonic earthquakes that nucleate via friction-dominated slip on planar surfaces.

1 INTRODUCTION

Compared to natural seismicity recorded near active faults by local arrays or borehole instruments, the volume of data is enormous (thousands of events per day) and the events are recorded close to the source (stations are located 50 m - 5 km from the events). In addition, mining-induced seismicity is unique because it includes events directly triggered by blasting that are assumed to involve fresh fracturing of rock as well as those induced over longer time scales that have been hypothesized to be dominated by frictional slip. These distinctions have so far been based on spatio-temporal clustering statistics and spectral signatures of these two types of events. Further clarification of the differences between these two types of events as well as documentation of their interactions is crucial for mine hazard analysis as well as for insight into the basic science of earthquake physics. The depth and magnitude range spanned by these events is comparable to borehole studies in California and to the target of the San Andreas Fault Observatory at Depth [SAFOD] drilling project that is currently in its beginning stages in the United States.

2 SOURCE PARAMETERS

We have assembled a dataset of large (M_w > 1.4) mining-induced events from four gold mines in the Far West Rand region. The locations of these events were determined by operators at the mines via a ray-tracing algorithm based on body wave arrival times (Mendecki, 1993, 1997). This method incorporates a layered velocity model based on geologic units that have been determined by underground surveying and mapping as well as surface-based refraction profiles and borehole log data. The wavespeeds and location procedures have been verified by test blasting, so location uncertainties are typically on the order of 10-20 m for events of M_w > 2.

Using the spectral method developed by Andrews (1986) and adapted by Richardson & Jordan (2002) for use with in-mine seismic recordings, we have calculated source parameters for fourteen events that occurred in 1999, and 23 events from 1998 (see Table 1). Each one of the events in this study was recorded by at least ten stations. In order to determine source parameters, we median-stacked each event's spectra and integrated the results up to the Nyquist frequency to determine S_D, the integral of the displacement power spectra (see Equation 6 of Andrews, 1986), S_V, the integral of the velocity power spectra (see Equation 7 of Andrews, 1986), and A^2, the acceleration power spectral level (see Equation 19 of Andrews, 1986). These are used to determine the source parameters radiated energy (E), seismic moment (M_0), and static stress drop ($\Delta\sigma$) as follows:

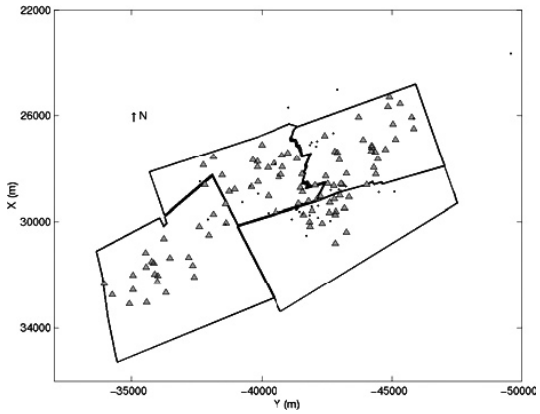

FIG. 1 **Map view of the lease areas of four mines in the Carletonville district (in mine coordinates). There are 102 three-component stations installed at depth (triangles). Dots represent the epicentres of large mining-induced events for which spectral source parameters were calculated (see Table 1) in this study**

$$E = 4\pi\rho v S_V$$

$$M_0 = \frac{8\pi\rho v^3 S_D^{(3/4)}}{\Re S_V^{(1/4)}}$$

$$\Delta\sigma = \frac{2\pi f_0 \rho A^2}{C\Re}$$

in which the corner frequency is found by

$$f_0 = \left(\sqrt{S_V / S_D}\right) / 2\pi.$$

In the previous equations, ρ is the rock density, which has been determined experimentally at the mines, v is wavespeed, $\Re$ is a constant based on the radiation pattern, and C is also a small constant. An advantage of this method is that the exponent of the spectral rolloff is not a fixed parameter as in the case of fitting spectra with a Brune-type curve. Because our data is band-limited, there is an upper limit to the radiated energy we can determine (Ide & Beroza, 2001). However, in practice the underestimation of energy for this dataset is very small (approximately 5%) since typical corner frequencies for the events in this study are generally 1/5 to 1/10 of the Nyquist frequency (Richardson & Jordan, 2002).

In Table 1, event dates and times are listed as yyyymmddhhmmss (The event times are local to the mines. Subtract two hours to obtain GMT time). Event locations are given by their latitude (°N), longitude (°E), and depth (meters below datum). It should be noted that event depths are referenced to the origin or "datum" of the Z axis of the local mine coordinates. This datum is a reference point in Johannesburg, and is 250 m above ground level and about 1800 m above sea level in the Carletonville Mining District where these events occurred. Seismic moment M_0 is in Nm, magnitude M_w is moment magnitude (Hanks & Kanamori, 1979), energy E is given in Joules, corner frequency f_0 is in Hz, and static stress drop $\Delta\sigma$ is in MPa.

3 MOMENT TENSORS OF SELECTED EVENTS

We determined moment tensors for events that covered a range of magnitudes, depths, and locations to provide as much variation as possible in composing a catalog of "typical" large mining-induced events. Some events are also part of foreshock-mainshock-aftershock sequences. We followed the method outlined in Ammon et al. (1998) and calculated regional Green's functions, then inverted for the moment tensors using broadband data from the Kaapvaal PASSCAL deployment. Since we used the PASSCAL data alone, we obtained independent measurements from those of the in-mine array data previously used to determine the source parameters (see Table 1). A comparison of event magnitudes as calculated by the spectral method using only the in-mine array data with magnitudes determined as part of the moment-tensor inversion is shown in Figure 3. By only using eight nearby stations for the inversions (see Figure 2), we will be able to use the more distant stations for regional phase amplitude analysis; therefore, the results of the two studies will not be dependent upon each other.

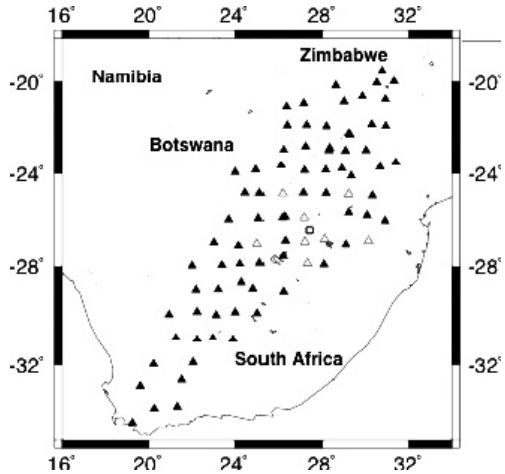

FIG. 2 Map of southern Africa showing locations of the Kaapvaal Craton PASSCAL deployment (triangles). Grey triangles are the stations used in the moment tensor inversions. The small box is the area shown in detail in Figure 1

To compute regional Green's functions, we used a simple 45-km thick crustal half-space for the velocity model based on the results of receiver function analysis of the crustal structure of the Archean craton by Nguuri et al. (2001). This study determined that crustal thickness ranged from approximately 41-50 km across the area covered by the stations used in our moment tensor inversions. We used wavespeed and density values determined experimentally by the mines (P = 6.1 km/s, S = 3.65 km/s, ρ = 2.7g/cm^3).

The results of the moment tensor inversions are given in Table 2. These are fully deviatoric tensors. We allowed the moment tensors to have some isotropic component in the inversion, but none were significantly isotropic. This result may be a bit surprising, since previous studies have shown that many large mining-induced events have significant implosive volumetric components (McGarr, 1992). It has been shown that S/P-wave amplitude ratios of mining-induced events are often smaller for events with significant isotropic components when compared with purely double-couple events of approximately the same moment (Cichowicz et al., 1990, Gibowicz et al., 1991). Therefore, we calculated the S/P-wave amplitude ratios of several other events between $1 < M_w < 2$ whose signal-to-noise ratios were not good enough to perform moment tensor inversions using broadband data. The S/P-wave amplitude ratios were not significantly different than those of the double-couple events for which we determined moment tensors, and therefore we do not expect significant isotropic components of the source down to at least $M_w = 1$. It should be noted that the previous studies involving S/P-wave amplitude ratios were conducted with events of $M_w < 0$.

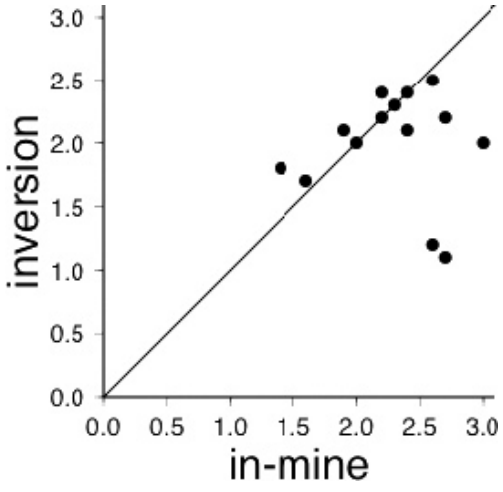

FIG. 3 Comparison between moment magnitudes as determined by the spectral analysis using in-mine seismic data and that determined through the moment tensor inversion using the broadband data. The 1:1 line is drawn for reference

The fourteen events for which we determined moment tensors ranged in size from $1.4 < M_w < 3.0$ and ranged in depth from 1.6 km to 3.8 km. This depth range is typical of the larger mining-induced events in the Carletonville district. We do not observe any significant trend in type of faulting with either depth or event size (see Figure 4).

The events in this study so far show two major modes of failure: normal faulting and strike-slip faulting. It is surprising to find such a large population of strike-slip events in this group, as the vast majority of faults observed underground have measurable offsets consistent with normal motion alone. There are several possibilities for this apparent discrepancy. Not all seismogenic faults are directly visible

underground, therefore there may be a historical bias in favor of normal faults because of observational limitations. In addition, the faults observed underground have yet to be studied in detail to determine whether all fault offset is due to seismic activity, or whether there is some creep. For example, do faults creep in a normal sense, but release seismic energy in a strike-slip or dip-slip pattern? Strike-slip motion is inherently difficult to discern when there is only limited visible access and when the displacement is not large enough to juxtapose different formations. There has been little in the way of detailed analysis of fault cores taken from depth; therefore sense of motion has been assumed, but may in fact be a relic of ancient fault activity that predates the active mining. It may also be that these moment tensors, which were determined by surface broadband data alone, are not accurate, although the waveform fits are generally good. We have not correlated any underground shear zones with the events in this study. In addition, we did not consider the effects of possible mislocations or errors introduced from noisy recordings, which could have significant effects on the moment tensor inversion results (Trifu et al., 2000). Clearly, in order to confirm the validity of our results, we must add data from additional stations to ensure good focal sphere coverage, perform a joint inversion using in-mine data, and include S-wave data in our inversions. However these next steps are beyond the scope of these preliminary results.

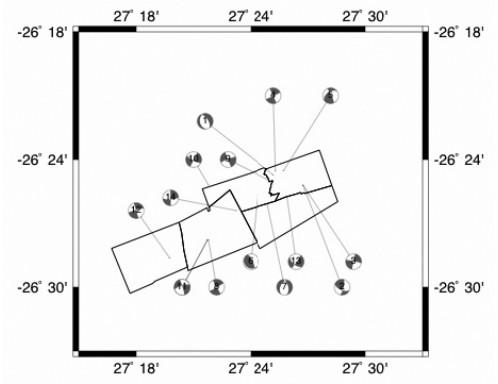

FIG. 4 **Map view of the lease areas of five mines in the Carletonville district with locations and beachball diagrams of the events for which moment tensors have been determined. Events are labelled in chronological order (The beachball labelled "1" is 19990103155836, and the beachball labelled "14" is 19990226143150, etc.)**

4 CONCLUSIONS

We have calculated source parameters for 46 mining-induced events of $M_w > 1$ and inverted for the best-fitting moment tensors for 14 of these events. We do not find any significant isotropic components of the source for any of the events studied. This supports the hypothesis that large mining-induced failures occur by shearing of pre-existing planes of weakness under frictionally-controlled conditions (i.e. high normal stress) and that these events are physically analogous to natural tectonic earthquakes. A surprising number of strike-slip mechanisms were determined, rather than all normal faulting, which was expected. There have been few thorough studies of the source characteristics of these events to date with which to compare our results. Therefore we must continue to determine more moment tensors, and we must incorporate the in-mine data in a joint inversion for the moment tensors. The next step in the characterization of these mining-induced events is to determine regional energy partitioning and propagation. The results of this work should allow further comparison between these events and naturally occurring tectonic events.

ACKNOWLEDGMENTS

This research was sponsored by the National Nuclear Security Administration, the Office of Nonproliferation Research and Engineering, and the Office of Defense Nuclear Nonproliferation under Contract No. DE-FC03-02SF22673 (E.R. and A.N.) and Contract No. W-7405-ENG-48 (W.W. and A.R.) The authors would like to thank Chuck Ammon for lending his expertise in calculating regional Green's functions.

REFERENCES

Ammon, C.J., Herrmann, R.B., Langston, C.A. and Benz, H. (1998) Source parameters of the January 16, 1994 Wyomissing Hills, Pennsylvania earthquakes. Seism. Res. Letters 69, pp. 261-269.

Andrews, D.J. (1986) Objective determination of seismic source parameters and similarity of earthquakes of different size. In Earthquake Source Mechanics (eds. S. Das, J. Boatwright, C.H. Scholz) vol. 6 of Geophysical Monograph 37, Am. Geophys. Union, pp. 259-267.

Cichowicz, A., Green, R.W.E., van Zyl Brink, A., Grobler, P. and Mountfort, P.I. (1990) The space and time variation of micro-event parameters occurring in front of an active stope, in Rockbursts and Seismicity in Mines, (ed. C. Fairhurst) vol. 2, pp. 171-175.

Gibowicz, S.J., Young, R.P., Talebi, S., and Rawlence, D.J. (1991) Source parameters of seismic events at the Underground Research Laboratory in Manitoba, Canada: Scaling relations for events with moment magnitude smaller than –2, Bull. Seism. Soc. Am. 81, pp. 1157-1182.

Hanks, T.C. and Kanamori, H. (1979) A moment magnitude scale, J. Geophys. Res. 84, pp. 2348-2350.

Ide, S. and Beroza, G.C. (2001) Does apparent stress vary with earthquake size?, Geophys. Res. Lett., 28, pp. 3349-3352.

Mendecki, A.J., ed. (1997) Seismic Monitoring in Mines, Chapman and Hall.

Mendecki, A.J. (1993) Real time quantitative seismology in mines, Keynote lecture in Proc. 3rd Intl. Symp. on Rockbursts and Seismicity in Mines, (ed. R. P. Young) Balkema, Rotterdam, pp. 1141-1144.

McGarr, A. (1992) Moment tensors of ten Witwatersrand mine tremors, Pure Appl. Geophys. 139, pp. 781-800.

Nguuri, T.K., Gore, J., James, D.E., Webb, S J., Wright, C., Zengeni, T.G., Gwavava, O., Snoke, J.A. and Kaapvaal Seismic Group (2001) Crustal structure beneath southern Africa and its implications for the formation and evolution of the Kaapvaal and Zimbabwe cratons, Geophys. Res. Lett. 28, pp. 2501-2504.

Richardson, E. and Jordan, T.H. (2002) Seismicity in deep gold mines of South Africa: Implications for tectonic earthquakes, Bull. Seism. Soc. Am. 92, pp. 1766-1782.

Trifu, C.-I., Angus, D. and Shumila, V. (2000) A fast evaluation of the seismic moment tensor for induced seismicity, Bull. Seism. Soc. Am. 90, pp. 1521-1527.

TABLE 1 Source parameters of mining-induced events determined from in-mine array data. Events for which moment tensors have been determined are shown in bold

Event	Lat	Lon	Depth	M_0	M_w	E	f_0	$\Delta\sigma$
19980111144841	-26.401	27.411	2338	1.4e13	2.7	5.5e8	15.8	5.87
19980220050356	-26.429	27.430	3694	7.8e13	3.2	1.0e10	12.9	20.00
19980328134551	-26.437	27.417	2729	1.2e13	2.7	2.8e8	16.6	3.65
19980329051801	-26.435	27.422	2587	2.2e13	2.8	4.9e8	16.3	3.46
19980331135629	-26.439	27.380	2053	2.2e13	2.8	2.1e8	9.3	1.47
19980404190603	-26.430	27.399	2047	1.1e13	2.7	1.8e8	14.6	2.51
19980420170707	-26.395	27.430	2273	2.8e13	2.9	1.6e9	13.8	8.76
19980420194749	-26.412	27.422	1925	2.5e13	2.9	9.1e8	14.8	5.72
19980502123739	-26.414	27.419	1955	2.2e13	2.8	4.9e8	11.9	3.43
19980508103233	-26.440	27.427	2661	1.1e13	2.6	1.8e8	12.1	2.46
19980622162025	-26.439	27.423	2588	1.3e13	2.7	3.4e8	15.2	4.01
19980708212049	-26.434	27.416	2553	1.2e13	2.7	3.9e8	14.8	4.83
19980727135740	-26.427	27.419	2409	2.5e13	2.9	4.3e8	9.5	2.73
19981002194336	-26.432	27.423	2569	1.0e13	2.6	1.3e8	10.2	1.90
19981007192539	-26.420	27.406	3123	2.0e13	2.8	1.3e9	16.9	10.30
19981019200410	-26.436	27.416	2505	1.3e13	2.7	2.0e8	10.5	2.40
19981021044841	-26.434	27.420	2613	1.0e13	2.6	1.3e8	11.5	2.00
19981023160058	-26.437	27.420	2745	3.1e13	2.9	7.1e8	8.7	3.50
19981027090946	-26.426	27.377	2989	1.2e13	2.7	3.6e8	15.2	4.72
19981102163835	-26.427	27.434	2552	2.5e13	2.9	6.2e8	10.4	3.90
19981110172424	-26.404	27.459	2770	1.2e13	2.7	3.1e8	15.0	4.10
19981119170822	-26.414	27.422	2268	1.1e13	2.6	3.0e8	13.3	4.20
19981223093859	-26.433	27.393	3375	2.8e13	2.9	1.1e9	12.8	5.94
19990103155836	**-26.412**	**27.420**	**1748**	**1.1e13**	**2.6**	**1.2e7**	**12.1**	**0.87**
19990118102526	**-26.420**	**27.446**	**3422**	**9.0e11**	**1.9**	**9.4e6**	**27.3**	**0.80**
19990118112405	**-26.420**	**27.446**	**3443**	**2.0e11**	**1.4**	**1.1e6**	**36.1**	**0.68**
19990118200717	**-26.415**	**27.422**	**2039**	**2.9e12**	**2.2**	**1.9e7**	**15.9**	**0.51**
19990118213352	**-26.409**	**27.429**	**2879**	**9.1e12**	**2.6**	**1.6e7**	**15.0**	**1.00**
19990201194832	**-26.428**	**27.406**	**3137**	**4.8e12**	**2.4**	**3.4e7**	**13.6**	**0.53**
19990202123021	**-26.435**	**27.415**	**2582**	**1.2e13**	**2.7**	**3.2e7**	**13.6**	**3.00**
19990203221201	**-26.423**	**27.363**	**2638**	**1.4e12**	**2.0**	**1.5e7**	**23.4**	**1.98**
19990205025535	**-26.420**	**27.417**	**2991**	**4.3e12**	**2.3**	**5.8e7**	**17.6**	**1.37**
19990205175933	**-26.420**	**27.363**	**2686**	**3.1e11**	**1.6**	**5.0e6**	**44.3**	**3.07**
19990205205457	**-26.463**	**27.362**	**2558**	**2.9e12**	**2.2**	**3.1e7**	**18.5**	**0.96**
19990209154922	-26.477	27.329	2738	6.6e11	1.8	3.1e5	10.7	0.19
19990209195821	**-26.401**	**27.418**	**1618**	**4.2e13**	**3.0**	**9.2e8**	**9.3**	**3.20**
19990216053511	**-26.429**	**27.432**	**3761**	**1.2e13**	**2.7**	**9.2e6**	**10.4**	**0.56**
19990226143150	**-26.397**	**27.387**	**1981**	**4.5e12**	**2.4**	**2.2e6**	**12.3**	**0.53**
19990309161938	-26.435	27.415	2464	1.1e13	2.6	6.8e7	8.1	0.99
19990310023001	-26.429	27.428	2651	1.0e13	2.6	1.7e8	14.9	2.50
19990318193538	-26.428	27.396	395	4.6e13	3.1	1.5e9	11.5	5.20
19990703111216	-26.169	27.497	3099	2.2e13	2.9	1.8e8	18.5	10.60
19990709200228	-26.395	27.413	7235	5.5e13	3.1	9.7e8	8.7	4.00
19990718173016	-26.393	27.403	3823	7.0e13	3.2	1.2e9	8.6	4.80
19990907150924	-26.386	27.446	3634	4.0e13	3.0	2.7e9	13.0	10.90
19990923132820	-26.386	27.452	4028	4.1e13	3.0	1.5e9	13.3	10.30

TABLE 2 Moment tensors of mining-induced events

Event	Mxx	Myy	Mxz	Myy	Myz	Mzz
19990103155836	-0.00027	-0.0027	0.0023	-0.0058	0.0022	0.0061
19990118102526	0.62	-1.21	0.018	-1.52	0.55	0.90
19990118112405	0.83	-2.75	-0.0035	-1.66	-0.31	0.83
19990118200717	-1.32	-1.69	0.026	2.39	-0.097	-1.07
19990118213352	-0.38	-0.19	-0.017	0.62	-0.41	-0.23
19990201194832	0.019	0.15	-0.14	0.11	-0.27	-0.13
19990202123021	-0.12	-0.032	-0.014	0.28	-0.019	-0.16
19990203221201	-1.88	-1.54	-0.013	3.63	0.088	-1.75
19990205025535	1.35	1.94	-0.096	-2.4	0.31	1.06
19990205175933	0.74	-0.67	-0.023	-1.23	0.14	0.50
19990205205457	0.41	0.90	-0.076	-0.97	0.32	0.56
19990209154922	-0.61	-1.43	0.056	1.21	-0.24	-0.60
19990216053511	0.0035	-0.0013	-0.0027	-0.0036	0.0016	7.38e-5
19990226143150	0.0041	-0.92	-0.046	0.19	0.28	-0.19